# MEASUREMENT ERRORS IN ROTATIONAL SYNTHESIS AND THEIR EFFECTS IN THE MAP PLANE

*(Invited paper)*

J.P. Hamaker
Netherlands Foundation for Radio Astronomy
Dwingeloo, the Netherlands

SUMMARY

The effect of errors in an aperture synthesis map is intimately related to the geometry of the synthesis instrument and the properties of the two-dimensional Fourier transformation. This paper concentrates on E-W rotational synthesis, the simple geometry of which allows a systematic treatment. After some preliminary remarks about error statistics and tolerances, the relevant properties of the Fourier transformation in polar coordinates are first reviewed. A classification of error types as "global", "circular", "radial" or "local" is introduced, based on the geometry of the area in the aperture over which they are coherent. A few special errors not fitting into this classification are also discussed. The characteristics of the corresponding patterns in the synthesized beam are described and illustrated with computer simulations and real-life examples.

## 1. PROLOGUE

### 1.1. Introduction

In the most general context of this Colloquium, very little can be said about errors that is worth writing about. Although most of them spring from sources common to all observing systems, the distribution of the aperture points they affect is entirely determined by the array configuration and, consequently, so are the error patterns in the map. I shall therefore narrow the scope of my contribution to East-West rotational synthesis, using the Westerbork Telescope in its original 10 x 2 configuration (Baars et al. 1973; Högbom and Brouw 1974) as a representative example.

Furthermore, I shall confine myself to continuum observations. Multichannel observations, either line or polarisation, do not differ fundamentally; in practice many errors track between channels and cancel in the subtractions that are an inherent step in the reduction (Weiler, 1973; Rots, 1974; for an example see fig. 3.7. below). The difficulties of these observations are associated mainly with the properties of the



*C. van Schooneveld (ed.), Image Formation from Coherence Functions in Astronomy, 27–45.*

antenna elements (e.g. primary beam polarisation, standing waves) or with fundamental difficulties in synthesis (the missing short spacings), both of which are outside the scope of this paper.

Even with all these restrictions, classifying and describing the errors is by no means simple. One fundamental reason is that the two-dimensional Fourier and convolution integrals in polar coordinates are not separable; a direct consequence is that there is no such thing as a scaling theorem for the angular coordinate. These complications make it extremely difficult to visualise the workings of the Fourier transformation. Moreover, the effect of the convolution of error beams and source brightnesses is not always easy to predict, as illustrated by fig. 1.1.

All these difficulties together probably account for the virtual non existence of litterature to be reviewed on the subject. My presentation will be mostly based upon our experience with the Westerbork Telescope. Before starting, a few general remarks are in order.

## 1.2. The meaninglessness of statistics

In many fields of science, errors can be treated meaningfully in terms of the theory of stationary random processes. The assumption that this is also true in aperture synthesis is implicit in many discussions and statements about map errors. In fact, however, the non-stationarity of the important errors is perhaps their most prominent general property.

Since most errors are related, directly or indirectly, to weather influences, they are highly nonstationary in time. Sensitivity of the equipment to these influences differing from antenna to antenna, there is spatial nonstationarity along the array. As a result of this and of the relatively small number of independent error parameters, a few errors usually dominate the scene in a map; the conspicuous patterns they produce are again anything but stationary. It is meaningless to describe them in terms of the familiar averages and variances of random process theory.

The concept of *dynamic range* is sometimes introduced and vaguely defined as the ratio of peak to weakest detectable brightness or flux in a map. A proper definition must state *what* one wants to detect *where* in the map (and perhaps also what constitutes a "detection").

The only possibly sensible use of statistical averages is in a comparison of large sets of maps, e.g. those made by different instruments or by one instrument at different frequencies, as was done by Hinder and Ryle (1971) in predicting the performance of synthesis arrays as a function of their size.

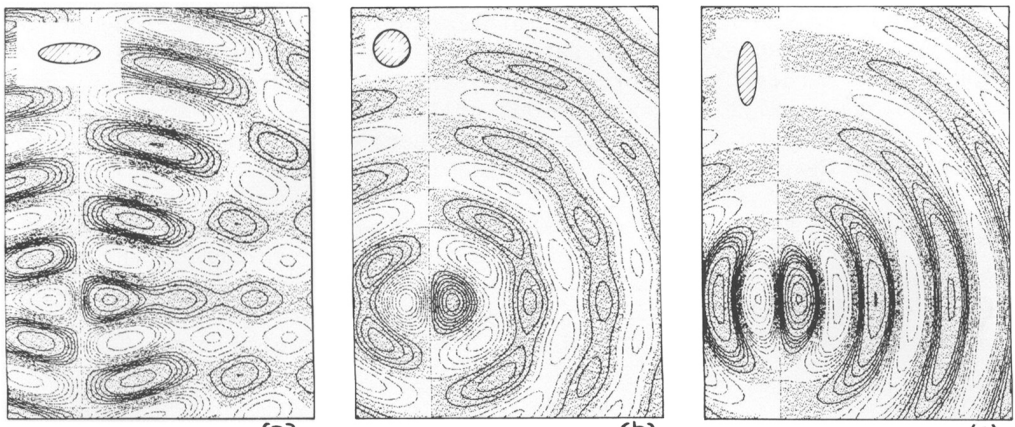


Fig. 1.1. The effect of convolving an error beam with a source distribution. Center: The error beam for an imaginary error $\Delta\varepsilon = 1$ in one interferometer; the circle indicates the half-power width of the corresponding interferometer beam $J_0(2\pi Rr)$ (cf. sec. 2.2.). Contour interval is 1%; positive areas are shown shaded. Left and right: The result of a convolution of this error beam with elliptical gaussian sources of half-power sizes as shown.

## 1.3. Tolerances for synthesis telescopes

The definition of tolerances is in a sense the inverse of error analysis, and therefore equally difficult for a synthesis instrument. What is specified usually reflects what is considered feasible, and is at best supported by some superficial computer simulations.

Stability goals in the order of 1% for gain and 1 mm for phase are typical and have proved to be adequate for important astronomical work in the lower GHz range. As observing frequencies are pushed up, more stringent phase specifications must be met in order to retain a good dynamic range. At the lower frequencies the same may become necessary for more subtle investigations in the wake of the earlier great discoveries.

The general properties of the source population must also be considered. At high frequencies sources are weaker with respect to receiver noise and relatively large beam errors may be tolerable. At low frequencies the field of view contains many more sources and observations become confusion-limited. For satisfactory "cleaning" a very tight control of error sidelobes is required.

## 1.4. Approach and layout of this paper

In the simple geometry of rotational synthesis, a reasonable approach

https://doi.org/10.1017/S0252921100074704 Published online by Cambridge University Press

is to consider the radial and azimuthal coherence of the various errors and the associated error beam patterns. (Note that I prefer the use of "coherence" rather than "correlation", which has a strong statistical connotation). Analytical expressions will be derived only where they are simple enough to be readily visualized. Where this is not the case, computer-simulated error pattern displays will be included.

Chapter 2 reviews the relevant properties of the two-dimensional Fourier transform. Chapter 3 discusses the various errors on the basis of a spatial coherence classification. Because of space and time limitations, the originally planned discussion of the more conventional processing methods of error control will be submitted elsewhere (Hamaker, 1979).

Terminology: The term *telescope* will be reserved for a synthesis *array* as a whole, the individual elements of which are the *antennas*. Both the separation vector of an interferometer and its length will be referred to as the *baseline*. The domain of the measured *complex visibilities* is the *aperture* (plane). The *map* is the image that is obtained by a two-dimensional Fourier transformation of the visibilities.

## 2. THE TWO-DIMENSIONAL FOURIER TRANSFORM

For the basic theory of Fourier transformations several excellent texts exist (e.g. Bracewell). I review here some of the specific aspects relevant to the present application.

### 2.1. Fundamental properties and assumptions

Symmetries. Brightness B being real, the visibility V is hermitian: $V(u,v) = V^{*}(-u,-v)$. An important consequence is that only one of each pair of points (u,v), (-u,-v) need be sampled; in rotational synthesis, a full observation lasts 12 rather than 24 hours. Re V, when transformed back, yields the *even* or *symmetrical* part of B; Im V reproduces the *odd* or *antisymmetrical* part.

"Energy". In the context of this paper this term may give rise to confusion. Physically, it is closely related to *flux* and *brightness*, whereas a common interpretation of certain theorems in Fourier theory relates it to the squares of these latter quantities. I shall use the term in its Fourier sense, retaining the quotes to remind you of the non-physical meaning to be attached to it.

The synthesized beam. With the standard assumption of *shift invariance stationarity* or *isoplanasy*, the telescope's effect in the output map is described by a convolution with a *synthesized beam*, which ideally is the transform of a *taper* function W. Errors modify the latter by multiplying it with an *error function* E. For the illustrations in this article, the standard Westerbork taper (a Gaussian with a value of 0.25 at the aperture

edge) will be assumed.

A few errors do not fit in the framework thus provided. They will be dealt with separately in sec. 3.5.

The error beam. The error function E should ideally be identically equal to 1. It is convenient to consider the *deviations*, that is, we write

$$E = 1 + \Delta g + i\Delta\varepsilon \qquad (2.1.1.)$$

and define the *error beam* $S_e$ as the transform of $W.(\Delta g + i\Delta\varepsilon)$. In a first-order approximation ($\Delta g$, $\Delta\varepsilon \ll 1$) we may identify $\Delta g$ with *gain* and $\Delta\varepsilon$ with *phase* errors. The small-error approximation $\Delta g$, $\Delta\varepsilon \ll 1$ will be used in most of this paper, although the displays of beam error patterns will be normalized to unity errors.

It is convenient to consider E as continuous, so that $S_e$ has no grating responses. One must remember, however, that such responses are generated through the convolution with the error-free beam. For those error patterns which are confined to a small area around the beam centre, the effects may be more conspicuous in the grating rings than in the central response.

## 2.2. The transform in polar coordinates

Using polar coordinates, the general Fourier transform relation between a map or beam pattern $P(R,\Phi)$ and its aperture counterpart $Q(r,\phi)$ reads

$$P(R,\Phi) = \int_{-\pi}^{\pi} d\phi \int_{0}^{\infty} rdr \;\; Q(r,\phi) \exp\left(2\pi i r R \cos(\Phi-\phi)\right) \qquad (2.2.1.)$$

(The projection factor $\sin\delta$ is not introduced here since it tends to obscure the inherent circular symmetries; it is better applied as a co-ordinate correction in the final result).

For the synthesized beam, the angular dependences disappear. The way the taper W(r) transforms into the beam S(R) can be visualised in two ways. Integrating over $\phi$ one gets

$$S(R) = 2\pi \int_{0}^{\infty} rdr\, W(r)\, J_0\,(2\pi r R), \qquad (2.2.2.)$$

showing S as a sum over all baselines of a series of circularly symmetric patterns with cross sections described by the zero-order Bessel function $J_0$. On the other hand, substitution of the one-dimensional Fourier

https://doi.org/10.1017/S0252921100074704 Published online by Cambridge University Press

transform

$$H(X) = \int_{-\infty}^{\infty} |r| dr\, W(r) \exp 2\pi i r X \qquad (2.2.3.)$$

into (2.2.1.) yields

$$S(R) = \int_{-\pi/2}^{\pi/2} d\phi\, H(R \cos\phi). \qquad (2.2.4.)$$

Thus S can also be viewed as the sum over all position angles of *"corrugations"* with cross sections H(X) (cf. Bracewell and Thompson 1973). These two quite different visualisations are relevant to the understanding of the effect of "circular" and "radial" errors, respectively (see Ch.3 below).

A more general relation which is sometimes useful is

$$\int_{-\pi}^{\pi} d\phi \cos n(\phi-\alpha) \exp (2\pi i r R \cos(\Phi-\phi)) =$$

$$= 2\pi i^n J_n(2\pi rR) \cos n(\Phi-\alpha). \qquad (2.2.5.)$$

For discrete radial sampling the pattern H(X) in (2.2.3.) becomes periodic, the repetitions giving rise to grating rings (Bracewell et al. 1973). The angular sampling is normally chosen dense enough to render its effects negligible.

## 2.3. Basic qualitative relationships between patterns in the two domains

Most of the relationships to be discussed here can be viewed as manifestations of the *scaling theorem* of Fourier theory. Qualitatively, this theorem states that the Fourier transform converts spatially extended patterns into narrow features and vice versa, while conserving the total "energy" in them. The precise meaning of "extended" and "narrow" is defined by the transformation formulae. I consider some examples.

The first is provided by fig. 2.1., which illustrates the familiar fact that a radial pattern transforms into another perpendicularly directed radial pattern. The same can be derived analytically from 2.2.3. and 2.2.4.

https://doi.org/10.1017/S0252921100074704 Published online by Cambridge University Press

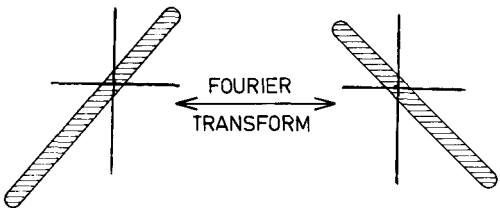


Fig. 2.1. See text

For stationary random noise, the power distribution in the beam is the transform of the autocorrelation function of the tapered error function E.W. and vice versa. If there is little correlation between error samples at different points, the autocorrelation function is concentrated in a narrow area and the beam noise is spread out widely. Also since the error "energy" is spread over the whole plane, the noise values in the beam are uncorrelated between points.

Upon the introduction of correlation between error samples the autocorrelation function widens, and consequently beam power concentrates toward the origin, while remaining uncorrelated between points. On the other hand, as one reduces the extent of the error distribution, the beam noise, while retaining the same extent, becomes more and more correlated between points. One manifestation of this is, that no noise "blobs" of dimensions smaller than the main response may occur anywhere in the synthesized beam, - a fact which is well-known in the analogous situation for a map.

Equation (2.2.2.) does not allow a simple interpretation in terms of the scaling theorem. It does indicate that circularly symmetrical features transform into patterns with similar symmetry, and is in this sense a counterpart to the radial pattern example above. More generally, (2.2.5.) indicates that angular modulation is conserved in the transformation. This also follows from elementary symmetry considerations.

## 3. ERRORS AND ERROR PATTERNS IN ROTATIONAL SYNTHESIS

In this chapter I consider the various types of errors in terms of the perturbations $\Delta g + i\Delta\varepsilon$ and the corresponding error beams $S_e$ (sec. 2.1.).

### 3.1. General classification

The errors may be grouped in various ways, e.g. according to their origin, magnitude, etc. Guided by the developments of the previous chapter, I choose to classify them on the basis of their coherence properties in the visibility plane (c.f. fig. 3.1.).

Global errors: Errors which coherently affect the whole aperture or a large part of it. Example: Clock errors.

https://doi.org/10.1017/S0252921100074704 Published online by Cambridge University Press

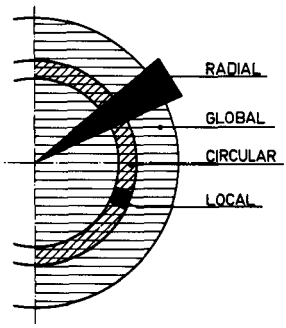


Fig. 3.1. Classification of error patterns in the aperture plane.

Radial errors: Errors coherent over a sector of the aperture; i.e. affecting many interferometers simultaneously over a limited period of time. Example: large clouds.

Circular errors: Errors coherent over large parts of circles in the aperture, i.e. affecting single interferometers over a sizable fraction of a full 12-hour period. Examples: Antenna position errors, electronic drifts.

Small-scale errors: Errors which are both short-lived and spatially confined, and therefore are incoherent in all directions in the aperture. Example: Small clouds.

## 3.2. Global errors

Coordinates. The orientation with respect to the source and the scale of the telescope baseline are affected by a considerable number of effects that are accurately predictable (precession, nutation, aberration, equation of equinoxes), measurable (observatory clock, polar motion, baseline in wavelengths), or (probably) small enough to be ignored at present (Earth tides).

I consider here two errors that are relatively difficult to calibrate accurately enough, and as a result frequently manifest themselves in Westerbork maps.

Clock errors result in map offsets in right ascension. When two or more observations with unequal offsets are combined, the most conspicuous effect is the incomplete cancellation of grating rings. The distortion of the main synthesized response becomes apparent when one tries to remove a strong point source from the combined map.

Tilts of the telescope as a whole with respect to the equatorial plane produce phase errors proportional to interferometer baseline. The map error consists of a slight source position shift and an antisymmetric East-West tail pair, see fig. 3.2.

https://doi.org/10.1017/S0252921100074704 Published online by Cambridge University Press

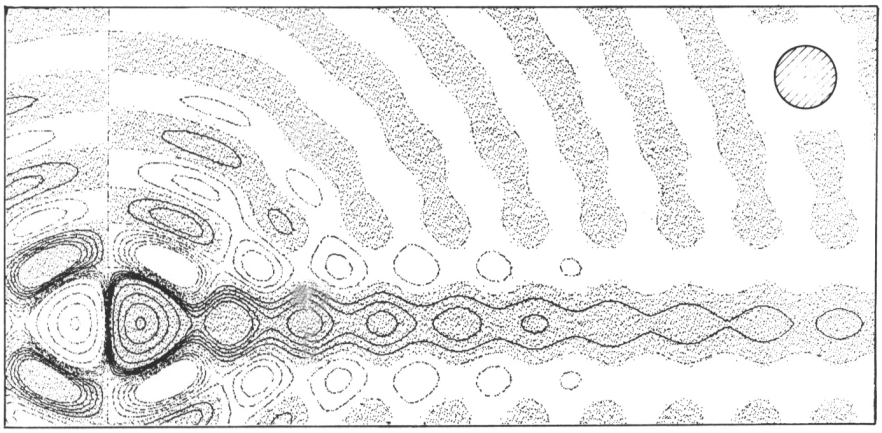

Fig. 3.2. The error pattern generated in a Westerbork beam by a baseline tilt out of the equatorial plane; the circle indicates the half-power size of the undisturbed beam. The pattern corresponds to errors $\Delta\varepsilon = r/r_{max}$ in the aperture. Contour levels are 0, $\pm$ 0.01, ...., $\pm$ 0.05, $\pm$ 0.10, ...., $\pm$ 0.25; positive areas are shown shaded.

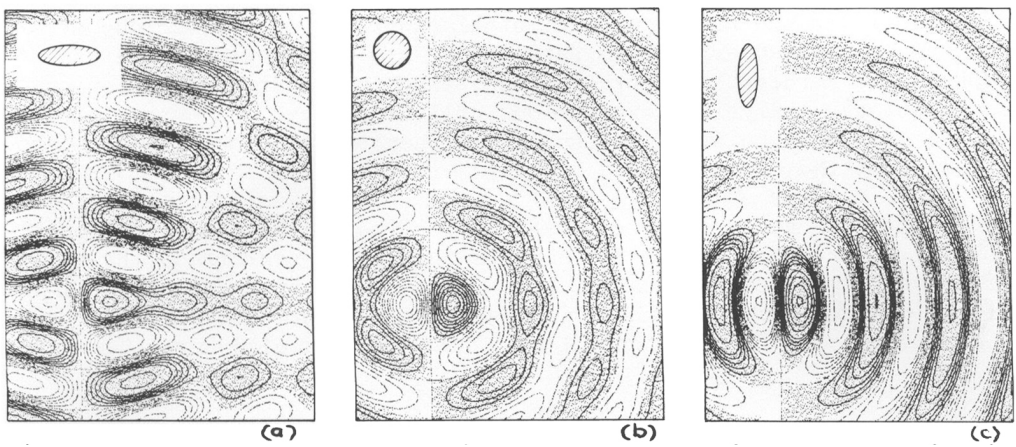


Fig. 3.3. The error pattern for sinusoidal gain errors $\Delta g = \cos(\phi + \alpha)$ in a single interferometer. Contour levels are the same as in fig. 1.1.

https://doi.org/10.1017/S0252921100074704 Published online by Cambridge University Press

Horizontally stratified atmosphere. The fundamental processes in the atmosphere are absorption, thermal radiation, refraction and Faraday rotation. For an atmosphere without horizontal structure, they affect the whole aperture coherently.

Absorption and radiation are proportional to path length and therefore vary with diurnal motion of the source. Since in most practical detectors output voltage is inversely proportional to some power of system temperature, the effect of radiation reinforces that of absorption; it becomes more pronounced as electronic receiver temperatures are reduced. Through variations of the effective gain of the whole telescope, these effects may again give rise to residual 12-hour grating rings, this time with even symmetry.

The magnitudes are dependent on the type of air mass through which one observes. At Westerbork for $\lambda = 6$ cm, zenith radiation temperature may change by some 5K and absorption by a few percent upon the passage of a weather front (J.D. Bregman, private communication). These numbers (and those for small-scale effects to be cited below) would certainly justify the effort of a systematic investigation. A treasure of relevant information should be available in the telecommunications litterature.

Refraction produces a differential effect due to the fact that for any position outside the meridian the two elements of an interferometer observe the source at unequal elevations. The effect can be quite adequately described in terms of a homogeneous slab troposphere with appropriate fixed parameters (Ryle and Elsmore 1973). At frequencies below 1 GHz ionospheric refraction must also be considered (Hinder and Ryle 1971).

Faraday rotation in the ionosphere is mentioned for completeness. It produces a rotation of observed polarisations but no beam distortions. For more information see Strom (1972).

### 3.3. Errors in individual interferometers - circular errors

A large number of error sources are associated with individual antenna elements. We first consider their effect in a single interferometer, deferring a discussion of correlations between interferometers to the end of the section. According to sec. 3.1., we need only consider time scales comparable to a full 12-hour observing period.

Deviations relative to the assumed geometry (position, axis orientation, inter-axis separation, gravitational bending) affect both phase and, in a shift-variant way through pointing errors, gain. The variations have a fundamental $2\pi$ period in hour angle.

Most other effects are associated, in one way or another, with the state of the ambient atmosphere. Thermal expansion of the antenna structure again affects the geometry, but in a not so neatly periodic way. Electronic circuits are sensitive primarily to temperature, whereas the

transmission of local oscillator signals is also influenced by pressure and humidity. Much can be done to suppress these influences, but the drifts with the longest time scales are particularly difficult to control. In the following I consider examples of error patterns to be expected as a result of such drifts.

A gain offset $\Delta g$ in an interferometer with baseline r is represented in the aperture plane by

$$E(r,\phi) = \Delta g \; . \; \delta(r) \qquad (3.3.1.)$$

and hence, according to (2.2.2.), results in an error beam

$$S_e(R) = \Delta g \; . \; 2\pi r \; W(r) \; J_o(2\pi rR). \qquad (3.3.2.)$$

24-hour sinusoidal phase error. Similarly, an error $i.\cos(\phi+\alpha)$ in an interferometer with baseline r produces an error beam (c.f. 2.2.5.)

$$S_e(R,\Phi) = \Delta\varepsilon \; . \; 2\pi r \; W(r) \; J_1(2\pi rR) \; \cos(\Phi+\alpha). \qquad (3.3.3.)$$

Note that the relation between the aperture and beam patterns is rotation-invariant, i.e. rotation of the error pattern in the "observed half" of the aperture imparts the same rotation to the beam.

Phase offset. In the above two examples, the required hermiticity of the errors is provided by elementary analytical expressions. For a phase offset, however, the aperture error becomes

$$E(r,\phi) = i\Delta\varepsilon \; . \; \mathrm{sgn}\,(\cos\phi). \qquad (3.3.4.)$$

The function sgn (cos $\phi$) is a square wave. Thus E may be expanded in an infinite Fourier series, each term of which can be transformed according to (2.2.5.). Alternatively, the transform can be shown to be related to $J_o(2\pi rR)$ through a horizontal line-by-line Hilbert transformation (Bracewell). Neither representation seems to be particularly useful.

The numerically evaluated beam is shown in fig. 1.1.(b). It exhibits the circular patterns one would have expected, but the structure within these is at first sight surprising. At closer inspection, one finds the maxima and minima to align, forming horizontal ridges and throughs of wave patterns which are associated with the pair of singularities at $(r,\pm\pi/2)$ in the aperture.

24-hour sinusoidal gain drift. The same difficulties are encountered in a treatment of a gain error $\Delta g.\cos(\phi+\alpha)$, which may serve as an appro-

https://doi.org/10.1017/S0252921100074704 Published online by Cambridge University Press

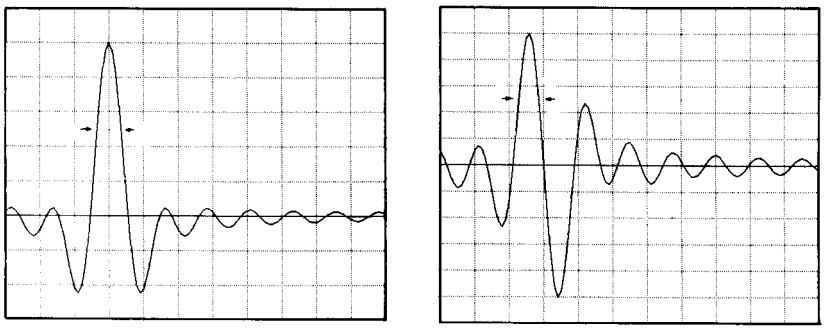

Fig. 3.4. The profiles H and $H_e$ (see text) for the standard Westerbork taper. The width of the circular synthesized beam is indicated by arrows.

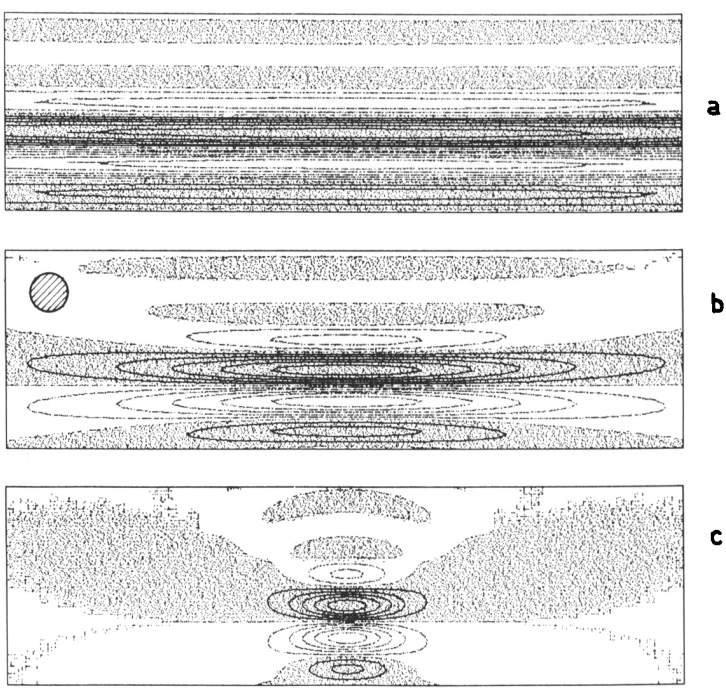


Fig. 3.5. Error beams corresponding to shifts in the apparent source position over prolonged periods of time. The shifts are assumed to produce phase errors $\Delta\varepsilon = (r/r_{max}) \exp(-\phi^2/\phi_o^2)$. From top to bottom the time span $\phi_o$ increases and, consequently, so does the maximum of the error beam. (a): $\phi_o$ = 6 min, contour interval $\Delta c$= .00125 x the peak value of the unperturbed beam: (b) $\phi_o$ = 22 min, $\Delta c$= .005; (c) $\phi_o$ = 90 min, $\Delta c$ = 0.02.

https://doi.org/10.1017/S0252921100074704 Published online by Cambridge University Press

ximation for drifts with a linear or quadratic time dependence. In the aperture

$$E(r,\phi) = \Delta g \cdot \cos(\phi+\alpha) \cdot \operatorname{sgn}(\cos\phi). \qquad (3.3.5.)$$

There is no rotation-invariance as for a sinusoidal phase error and the beam patterns are quite different for different values of $\alpha$, as shown in fig. 3.3. Horizontal wave patterns are discernible similar to that of fig. 1.1.(b), except for $\alpha = 0$, where the discontinuity in the visibility is of a higher order.

Higher harmonics. According to sec. 2.2. analytical transformations are possible for gain errors with frequencies of $2n/24h$ and phase errors at $(2n+1)/24h$. These transforms may be occasionally helpful but no new insights are involved.

Radial correlations. If an error occurs in a single antenna, it affects all the interferometers of which it is a member, thus introducing a correlation between errors at different radii in the aperture. The nature of these correlations depends entirely on the layout of the array.

Quite generally, the beams shown above have a wavy nature along map radii, the quasiperiod of the waves being inversely proportional to baseline. For an error occurring in two baselines simultaneously, two identical patterns with different quasiperiods are superimposed in the map, and we may expect beats to occur.

When a long-lived error occurs coherently in a considerable fraction of all interferometers, it is more properly classified as a global one. An example is provided by the secondary grating rings that frequently occur in Westerbork maps halfway between the radii of the standard 12-hour rings. They are associated with calibration errors in one of the movable antennas, which appear coherently in 10 simultaneous interferometers. Examples of a related error will be shown in sec. 3.5. The incomplete cancellation of regular grating rings (sec. 3.2.) can also be interpreted from this viewpoint. Since at the ring positions many interferometer responses add coherently, a very small error suffices to bring about a visible effect.

## 3.4. Atmospheric inhomogeneities - small scale and radial errors

Atmospheric inhomogeneities give rise to a distortion of the transmitted radiation wavefronts in addition to the effects already discussed in sec. 3.2. Such inhomogeneities occur both in the troposphere (primarily in water vapour concentration) and in the ionosphere (electron density). According to their size relative to the observing instrument they may be classified as "large" or "small".

https://doi.org/10.1017/S0252921100074704 Published online by Cambridge University Press

Small-scale irregularities. The effects associated with small irregularities are by definition confined to only a part of the telescope. Moreover, since irregularities are always associated with motion, they donot persist for long. The corresponding error function then consists of noise with an autocorrelation function that is narrow in both dimensions and thus, according to sec. 2.3, results in an extended low-level noise component in the error beam. Because of its noiselike character, the effect is difficult to assess in actual observations. In comparison with the large-scale errors presently to be discussed, the small-scale ones appear to be unimportant (Hamaker, 1978).

Large-scale phase irregularities. The existence of large-scale irregularities in ionospheric electron density has long been known. Recent work (Hardy 1974; Hargrave and Shaw 1978; Hamaker 1978) has revealed the frequent occurrence of refractive disturbances in the troposphere, with scale sizes spanning a range from about one to many tens of kilometers. According to the rate at which they move and/or change, they may persist for times ranging from minutes to hours or even the better part of a full half-day (Ryle and Elsmore 1973).

Being larger by definition than the telescope, these errors classify as "radial". Their primary effect is to shift the apparent instantaneous position of the source by an unpredictable amount, and the corresponding corrugation in (2.2.4.) undergoes a similar shift. The cross-section of the resulting error pattern is, in first order, given by

$$H_e(X) = \Delta X \cdot dH/dX \qquad (3.4.1.)$$

where H is the cross-section profile defined by (2.2.3.) and $\Delta X$ is the instantaneous position shift perpendicular to the corrugations, i.e. parallel to the telescope baseline. The cross-sectionsfor the Westerbork taper are shown in fig. 3.4. The main response is seen to consist of a positive-negative parallel ridge pair.

If the position shift persists for some time, these dual ridges are superimposed over the corresponding range of hour angles. Far out in the map, the result will tend to zero, positive and negative contributions neutralising each other. In the middle, all negative contributions coincide on one side of the beam centre, all positive ones on the other, so that constructive interference occurs. One thus finds a concentration and buildup of error power near the origin which becomes more pronounced as the error persists over a larger hour angle range; this is as it should be according to sec. 2.3. A computed example is shown in fig. 3.5., a practical example from Westerbork in fig. 3.6.

Absorption and radiation. The general remarks made in sec. 3.2. on our ignorance about these processes apply here as well. Small-scale effects noted at Westerbork are mostly associated with rain clouds, which, at 5 GHz in the zenith, produce antenna temperature variations of

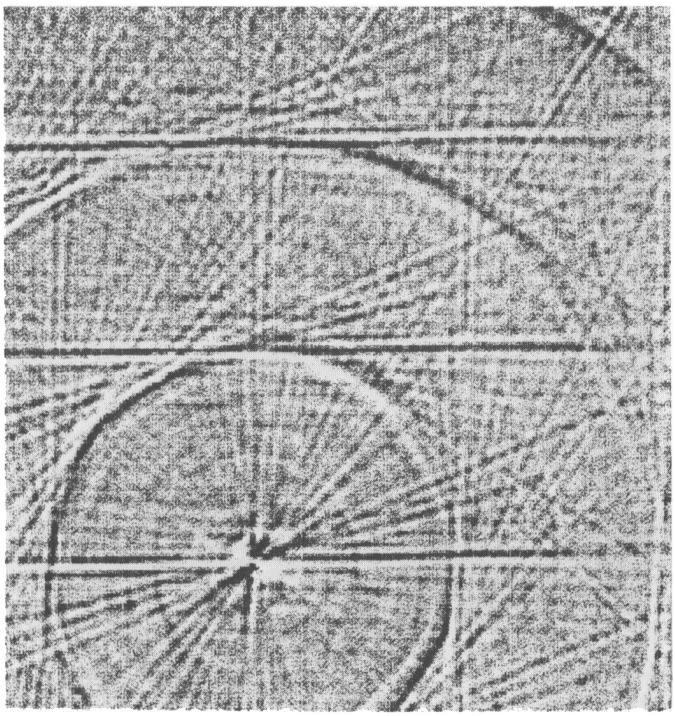

Fig. 3.6. The error beam for a 1x12 hr map of 3C48 made at Westerbork; large scale atmospheric refraction effects dominate the scene. Note the variety of radial extents corresponding to different time scales and the repetition at grating intervals. Near the position where the theoretical response was subtracted, error structures with even symmetry are seen which must correspond to gain errors in the observations.

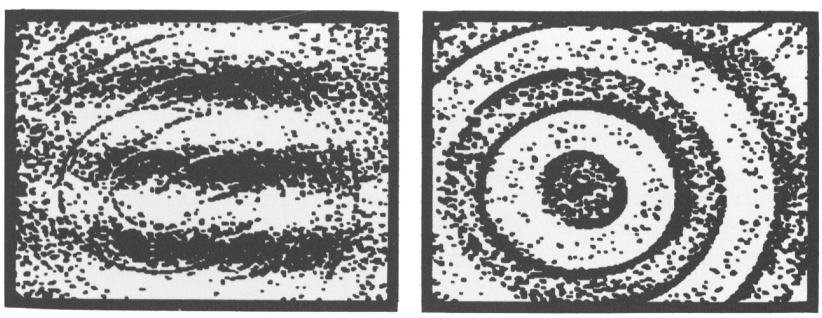

Fig. 3.7. (a) One-bit representation of a map of a single channel in a line observation at $\lambda$=21 cm made at Westerbork. The vertical-running wave pattern is due to cross-talk on the shortest baseline. (b) The same map with the continuum radiation (estimated from other channels) subtracted, demonstrating the ease with which many instrumental effects may be removed in a multichannel observation (courtesy R. Sancisi).

https://doi.org/10.1017/S0252921100074704 Published online by Cambridge University Press

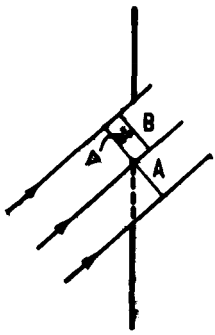


Fig. 3.8. Qualitative demonstration of the effect of shadowing for an off-axis source. For the unobstructed aperture, A is the phase centre. Under partial blocking (dashed line), this center shifts to B, receding over a distance Δ relative to the incident wavefront.

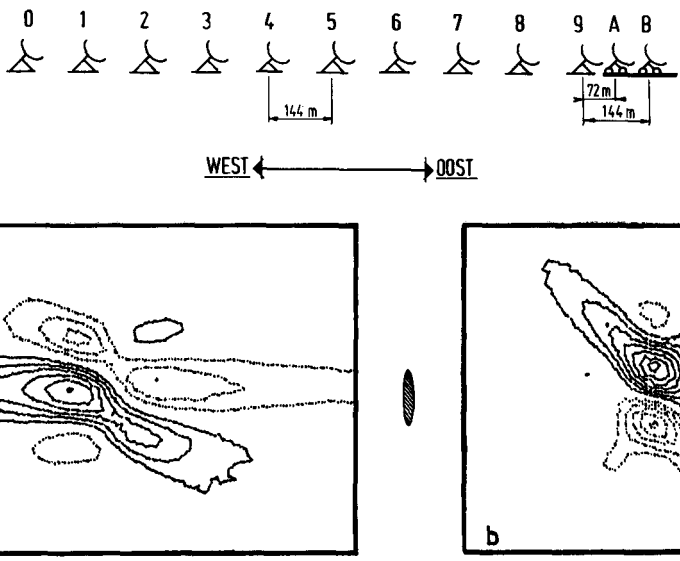


Fig. 3.9. Error beams caused by shadowing in a 12 hour observation with the Westerbork Telescope in the configuration shown. Declination is 10°. The source is at the 3 -dB point of the field of view (a) toward the right, contour interval 0.25% of synthesized beam maximum; (b) toward the top, contour interval 0.5%. The ellipse shows the half-power size of the synthesized beam. (Courtesy J.D. O'Sullivan)

the order of 5 to 10 K and signal power variations of several percent. Snow clouds are particularly heavy absorbers: Signal losses of 30% and antenna temperature rises of 100 K are typical, the phase at the same time remaining perfectly undisturbed (J.D. Bregman, private communication).

https://doi.org/10.1017/S0252921100074704 Published online by Cambridge University Press

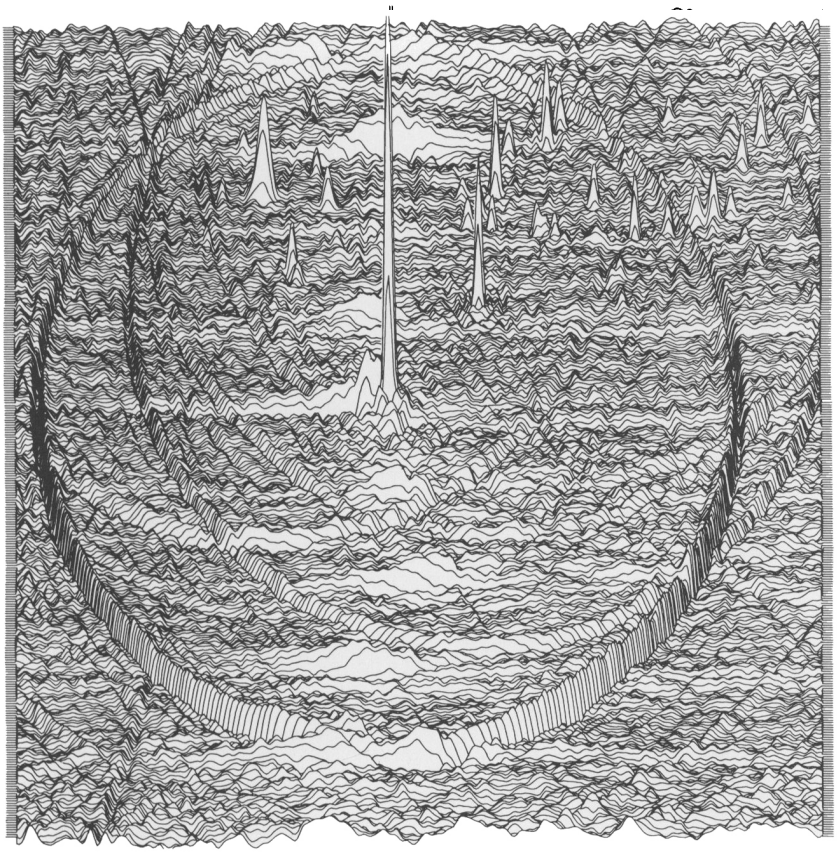

Fig. 3.10. Shadowing effects in a map of the Virgo cluster ($\delta=12^{\circ}$) at $\lambda=49$ cm. The field centre is near the top right corner. The map is made from two 12-hour observations, in which the distance between antennas 9 and A (cf. fig. 3.9.) was 36 and 72 metres, respectively. The strong grating rings thus correspond to a 36 m radial sampling interval of the aperture. (Courtesy C.G. Kotanyi.)

## 3.5. Mutual interference between antennas

It is unavoidable to put some antennas in close proximity to each other in order to sample the aperture plane as close as possible to the origin. Some peculiar effects result which are of considerable practical importance. Owing to their special nature, they can only be discussed outside the framework used so far.

https://doi.org/10.1017/S0252921100074704 Published online by Cambridge University Press

Cross-talk. For source directions close to the interferometer baseline vector, receiver noise radiated by an antenna nearer to the source may be picked up by the next antenna behind it. The picked-up signal has just the right amount of delay to produce an output when the signals from the two antennas are correlated. Since the effect only occurs for short baselines and hour angles close to $\pm \pi/2$, the corresponding map pattern consists of long "plane" waves "running" verically accross the map. Fig. 3.7 gives an example.

Shadowing. Under conditions similar to those for cross-talk, part of the aperture of one or more antennas becomes blocked or "shadowed" by another antenna in the line of sight. The loss of signal that results can easily be calculated; in a first-order approximation its shift-variance may be neglected and appropriate gain corrections applied.

It was recognized only recently that this is not the whole story. (J.D. O'Sullivan, unpublished). Indeed, for sources away from the field centre, the effective phase centre of the shadowed antenna shifts, as shown qualitatively by fig. 3.8. This shift is strongly dependent on source position in the observed field, and consequently, so are the error beams. Two calculated examples are shown in fig. 3.9. It is seen that shadowing is apt to produce artefacts that look just like the source tails which have aroused so much interest with astrophysicists.

An example from Westerbork is shown in fig. 3.10. It is seen that in this 2x12 hour observation the mock tail repeats at the AB grating interval. This is a clear sign that something is wrong; we owe its occurrence to the regularity of the layout of our array, combined with the fact that the shadowing environments for antennas A and B are different. For less regular arrays such as the VLA, such conspicuous warning signs may very well fail to occur.

Being strongly shift-variant, this effect is not easily corrected for. The procedure commonly used here is to simply delete all aperture points affected and restore the resulting map to a decent appearance through CLEANing. The CLEANed map might serve as a starting point for more refined iterative correcting procedures to be developed in the future.

ACKNOWLEDGEMENTS

I am indebted to W.N. Brouw, R.M. Forster, E. Raimond and G. Robertson for useful comments on earlier drafts of the manuscript, and in particular to the editor of this volume for very thorough screening of the final version. Miss W. Smit and Mrs. J.H. Millenaar were responsible for careful typework; the figures were prepared by R. van Dalen and H.W.H. Meijer. The Westerbork Synthesis Radio Telescope is operated by the Netherlands Foundation for Radio Astronomy with financial support from the Netherlands Organization for the Advancement of Pure Research.

REFERENCES

Baars, J.W.M., van der Brugge, J.F., Casse, J.L., Hamaker, J.P., Sondaar, L.H., Visser, J.J. and Wellington, K.J., Proc. Inst. Elec. Electron. Engrs. 61, 1258.
Bracewell, R.N., "The Fourier Transform and its Applications", New York: Mc Graw-Hill., 1965.
Bracewell, R.N. and Thompson, A.R., 1974, Astrophys. J. 182, 77.
Hamaker, J.P., 1978, to be published in Radio Science 13, Sept.-Oct. 1978.
Hamaker, J.P., 1979, to be submitted to Astron. Astrophys.
Hardy, R.N., 1974, Nature 249, 431.
Hargrave, P.J. and Shaw, L.J., 1978, Monthly Not. Roy. Astr. Soc. 182, 233.
Hinder, Richard and Ryle, Martin, 1971, Monthly Not. Roy. Astr. Soc. 154, 229.
Högbom, J.A. and Brouw, W.N., Astron. Astrophys. 33, 289.
Rots, A.H., 1974, Thesis, University of Groningen, Netherlands.
Ryle, M. and Elsmore, B., 1973, Monthly Not. Roy. Astr. Soc. 164, 223.
Schwarz, U.J., 1978, this volume.
Strom, R.G., 1972, Neth. Found. Radio Astr., Internal Techn. Rep. ITR-99.
Thompson, A.R. and Bracewell, R.N., 1974, Astron. J. 79, 11.
Weiler, K.W., 1973, Astron. Astrophys. 26, 403.

DISCUSSION (see also discussion after paper by Wilkinson-Readhead)

Comment J.R. FORSTER
Were the errors in visibility used to produce the error beams associated with antenna shadowing symmetrical in hour angle?
Reply J.P. HAMAKER
The shadowing effect itself is symmetrical in a sense, that is, the shadowing antenna at negative hour angles becomes the shadowed one at the other side of the meridian. However, since the antennas occupy different positions in the array (e.g. antennas 9 and A at Westerbork) the result in the aperture is by no means symmetrical, and this is reflected in the absence of any symmetry in the error beams.

Comment R.D. EKERS
Even if you have an error which is symmetrical the source may have a complicated asymmetric shape which when convolved with the error lobe will give an asymmetric result. In general it can be misleading to rely heavily on the expected shapes of error lobes for a point source if you have a field with extended objects.